frontiers | Frontiers in Nutrition

TYPE Systematic Review
PUBLISHED 29 August 2025
DOI 10.3389/fnut.2025.1644538

OPEN ACCESS

EDITED BY
Eric Gumpricht,
Independent Researcher, Gilbert, AZ, United States

REVIEWED BY
Phiwayinkosi V. Dludla,
University of Zululand, South Africa
Sontaya Sookying,
University of Phayao, Thailand

*CORRESPONDENCE
Fengming You
✉ youfengming@cdutcm.edu.cn
Jing Guo
✉ guojing19910307@sina.com

†These authors have contributed equally to this work and share first authorship

RECEIVED 12 June 2025
ACCEPTED 08 August 2025
PUBLISHED 29 August 2025

CITATION
Xiao X, Wu X, Li W, You F and Guo J (2025) Therapeutic effects and safety of resveratrol for lung cancer: an updated preclinical systematic review and meta-analysis. *Front. Nutr.* 12:1644538. doi: 10.3389/fnut.2025.1644538

Therapeutic effects and safety of resveratrol for lung cancer: an updated preclinical systematic review and meta-analysis

Xiang Xiao[1†], Xuanyu Wu[1†], Wenyuan Li[1,2], Fengming You[1,3*] and Jing Guo[1*]

[1]Hospital of Chengdu University of Traditional Chinese Medicine, Chengdu University of Traditional Chinese Medicine, Chengdu, China, [2]Evidence-Based Traditional Chinese Medicine Center of Sichuan Province, Chengdu, China, [3]Cancer Institute, Chengdu University of Traditional Chinese Medicine, Chengdu, China

Background: Lung cancer (LC) is the most common cause of cancer-related death worldwide, while there are limited treatment methods. Resveratrol (RESV), a natural food-derived compound, has attracted attention around the world for its anti-LC effects. However, little is known about the efficacy and safety of RESV for LC.

Purpose: This study aimed to provide preclinical evidence for the efficacy and safety of RESV for LC, and to find the optimal dose and duration.

Methods: *In vivo* studies of RESV against LC, published before 24 July 2024, were retrieved from PubMed, Embase, Web of Science, and Cochrane Library. The CAMARADES checklist was used to assess study quality. Primary outcomes were tumor volume and tumor weight. Secondary outcomes included body weight, lung metastases number, and the apoptotic cell proportion. Statistical analysis was performed using RevMan 5.3 and Stata 16.0. Dose–duration–effect model was conducted to determine the optimal dose and duration, and the toxicology of RESV was predicted through the ProTox 3.0 platform.

Results: A total of 23 studies involving 425 animals were included. The methodological quality of included studies was medium-to-low. RESV significantly reduced tumor volume, tumor weight, and lung metastases number, and increased apoptotic cell proportion, while having no effect on body weight. High heterogeneity was observed, and subgroup analysis suggested that the heterogeneity was partly attributed to the dose of RESV. The optimal dose and duration of RESV were 30–100 mg/kg and 25–28 days, respectively. The median lethal dose of RESV was 1,560 mg/kg.

Conclusion: RESV demonstrated a significant inhibitory effect on LC *in vivo*. However, the lower research quality and high heterogeneity call for more high-quality preclinical studies to be conducted. Before achieving clinical translational research on RESV, the problem of low bioavailability of RESV needs to be solved.

KEYWORDS

lung cancer, resveratrol, preclinical evidence, systematic review, meta-analysis

Introduction

Lung cancer (LC) led to 1,817,172 deaths in 2022, and remains the most common cause of cancer-related death (18.7% of total deaths), resulting in an enormous global social and economic burden (1). The disastrous prognosis of LC is largely due to factors, including late-stage diagnosis (2), acquired drug resistance, and low treatment tolerance (3), which significantly impede effective treatment and contribute to the high mortality rate. Indeed, various treatment strategies, including surgery, chemotherapy, radiotherapy, targeted therapy, and immunotherapy, have moderately improved survival outcomes in patients with LC. Yet, the overall prognosis remains poor, and the estimated 5-year survival was only 26.4% (4). Additionally, existing pharmacological treatments exhibit significant limitations. Chemotherapy is associated with notable adverse effects, including neurotoxicity, gastrointestinal disturbances, and cardiovascular toxicity (5). Targeted therapies are applicable to a specific subset of patients and are prone to inducing adverse reactions such as irreversible pulmonary fibrosis (6). Immunotherapy is effective for only a limited population and is frequently accompanied by the development of acquired resistance (7). Consequently, there is an urgent need to identify and develop efficacious, tolerable, and safe therapeutic strategies for LC.

Identifying compounds with anticancer activity in natural foods has been a topic of interest for years. Resveratrol (RESV), a phenolic compound found in many plants such as grapes, blueberries, and peanuts, exhibits various pharmacological and biological activities, including anti-aging, anti-inflammatory, antioxidant, antifibrotic, and anticancer effects (8, 9). Indeed, RESV has shown potential in treating a wide range of cancers, including lung, breast, colorectal, renal, liver, and bladder cancers (10–15) (Figure 1). In clinical trials, RESV has demonstrated promising properties for colorectal, breast, and prostate cancers (16). Unfortunately, no clinical study has yet confirmed whether RESV is effective in patients with LC, although numerous *in vivo* and *in vitro* studies have explored its anti-LC effects. *In vitro*, RESV treatment increased the chemical sensitivity of A549 cells to cisplatin (10). *In vivo,* RESV can inhibit LC progression by suppressing the activation of tumor-associated macrophages (17). Nevertheless, the protective effect of RESV against LC in animals has not been systematically reviewed, and its mechanism remains unknown.

A systematic review and meta-analysis of preclinical studies provides valuable insights into the reliability of preclinical studies and facilitates the transition from animal to clinical trials (18). The absence of clinical trials investigating RESV for LC treatment currently precludes robust evaluation of its therapeutic efficacy and safety in human patients. Nevertheless, a comprehensive meta-analysis of preclinical studies may yield valuable therapeutic insights and critical preliminary guidance for future clinical translation. A meta-analysis published in 2016 reported RESV significantly reduced the incidence of LC by 36% *in vivo* (19). With the publication of numerous studies

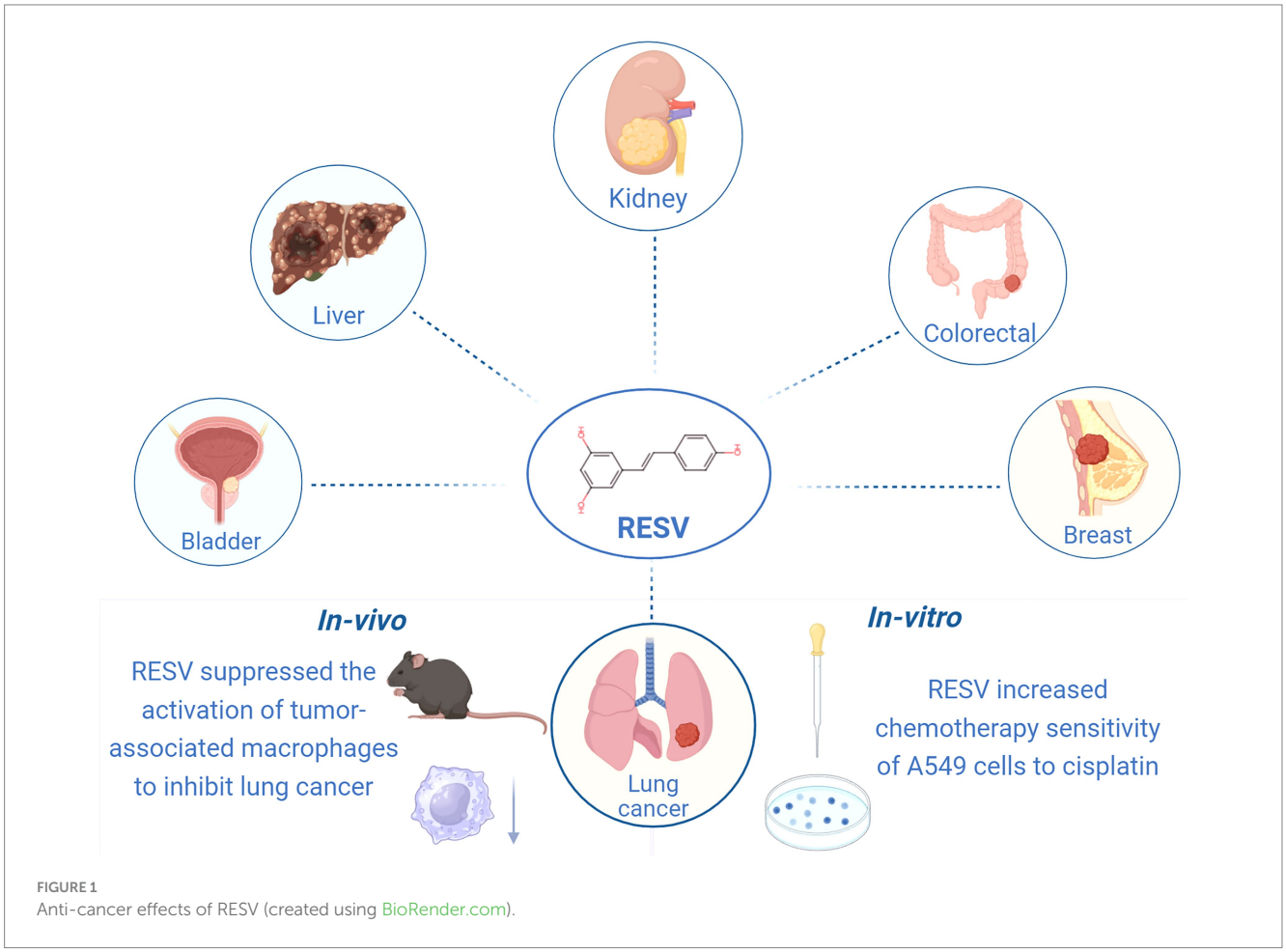

FIGURE 1
Anti-cancer effects of RESV (created using BioRender.com).

focusing on RESV against LC, it is necessary to conduct an updated meta-analysis to improve the accuracy of estimated effects. Herein, we systematically reviewed the effects of RESV in LC animals in order to provide preclinical evidence for subsequent clinical trials. We hope RESV may become a promising natural treatment for LC in the future.

Materials and methods

Study registration

This study followed the Preferred Reporting Items for Systematic Reviews and Meta-Analyses (PRISMA) guideline (20), and has been registered on PROSPERO (CRD42024569393).

Search strategy

PubMed, Embase, Web of Science, and the Cochrane Library were searched by two authors (Xiang Xiao and Xuanyu Wu) to identify relevant studies. The search period was from the establishment of the database to 24 July 2024. The search was carried out by using MeSH combined with free words (Supplementary Table 1). Additionally, we searched the references of included studies to collect other potential studies.

Study selection

Two authors (Xiang Xiao and Wenyuan Li) selected studies following the PRISMA guidelines using EndNote X9 software. Selection results were cross-checked to ensure consistency, and a third investigator (Jing Guo) was consulted to resolve disagreements. We screened titles and abstracts to exclude irrelevant and non-English studies after duplicate papers were eliminated through electronic and manual-based steps. Full texts of the remaining studies were then reviewed to confirm final eligibility.

Based on the PICOS principle, the inclusion criteria were as follows: (1) participants (animals): LC model animals, including orthotopic tumors and ectopic transplanted tumors, without limitation of species, sex, or age; (2) intervention: the intervention group was treated with RESV, and the dose and duration were clarified; (3) comparator: the control group was treated with placebo or saline; (4) outcome measure: the primary outcomes were tumor volume and tumor weight, and the secondary outcomes were lung metastases number, body weight, and apoptotic cell proportion; and (5) study design: only *in vivo* animal studies with separate treatment groups were eligible.

The exclusion criteria were as follows: (1) studies that were not *in vivo* animal studies, such as clinical studies, *in vitro* studies, *in silico* studies, reviews, letters, conference papers, abstracts, and editorials; (2) studies with missing data; (3) studies in which the intervention group received RESV derivatives or analogs; and (4) studies without any pre-set outcomes.

Data extraction

Two authors (Xiang Xiao and Xuanyu Wu) extracted the following information independently using Excel 2021 software: (1) article information, including first author's name, publication year, and country; (2) animal information, including species, sex, age, and weight; (3) modeling information, including modeling method, drug/cell, route, dose, duration, and anesthetic; (4) intervention information, including dose, duration, and route; (5) sample size of both intervention and control groups; and (6) mean and standard deviation (SD) of outcome measures (final time point result). The WebPlotDigitizer[1] was employed to measure graphic values. The *p*-values not reported in studies were calculated using the independent samples t-test (summarized data) function in the SPSS 26.0 software. An investigator (Xiang Xiao) contacted the corresponding authors to get missing data.

Risk of bias assessment

The 10-item CAMARADES checklist (21) was employed by two authors (Xiang Xiao and Wenyuan Li) independently to evaluate the quality of included studies. The assessment criteria were as follows: (1) peer reviewed publication; (2) control of temperature; (3) random allocation to treatment or control; (4) blinded induction of ischemia; (5) blinded assessment of outcome; (6) use of anesthetic without significant intrinsic neuroprotective activity; (7) animal model (aged, diabetic, or hypertensive); (8) sample size calculation; (9) compliance with animal welfare regulations; and (10) statement of potential conflict of interests. Each item was evaluated at "high," "low," or "unclear" risk based on the information reported in the full text and Supplementary materials.

Dose–duration–effect 3D model

The Origin 2021 software was used to display 3D models of the dose and duration of RESV and the primary outcome measures (tumor volume and tumor weight).

RESV toxicology prediction

The toxicity assessment of RESV was insufficient in the included studies. Herein, ProTox 3.0,[2] an online platform, was employed to predict the toxicology of RESV. The organ toxicity, carcinogenicity, immunotoxicity, mutagenicity, cytotoxicity, blood–brain barrier (BBB) permeability, ecotoxicity, clinical toxicity, and nutritional toxicity were predicted.

Statistics analysis

The RevMan 5.3 and Stata 16.0 were used for meta-analysis. The weighted mean difference (WMD) and 95% confidence interval (CI) were used when comparing continuous variables with consistent measurement methods and units across studies; otherwise, the standardized mean difference (SMD) and 95% CI were applied.

1 https://automeris.io/login/

2 https://comptox.charite.de/protox3/

Heterogeneity was assessed using the I^2 statistic and Cochrane's Q test. Heterogeneity was graded as high ($I^2 > 75\%$), moderate ($50\% \leq I^2 \leq 75\%$), or low ($I^2 < 50\%$). For Cochrane's Q test, a p-value < 0.05 indicates significant heterogeneity. When high or moderate grade heterogeneity was observed, we first performed sensitivity analysis by sequentially removing each trial to determine if any single study contributed to the heterogeneity. If substantial heterogeneity in tumor volume persisted and its source remained unexplained after sensitivity analysis, subgroup analysis or meta-regression was performed to explore potential causes. Subgroup analysis was stratified by the dose of RESV (22). Meta-regression analysis identified eight variables as potential sources of heterogeneity: publication year, dose, duration, administration, modeling method, species, gender, and region. Variables with a p-value < 0.05 were considered significant contributors to heterogeneity. For low-grade heterogeneity, we used a fixed-effect model to combine effect sizes; otherwise, a random-effects model was employed. Funnel plots and Egger's regression test were conducted to explore publication bias when there were more than 10 studies.

Results

Search and selection results

A total of 2,261 records were obtained through database screening, and 1,690 records were obtained after eliminating duplicates. After reading titles and abstracts, 260 records remained. After reviewing the full text of the 260 articles, 23 studies were ultimately included for meta-analysis. For different subgroups present in a study, we treated them as different experiments, and among the 23 studies, there were 30 experiments (Figure 2).

Characteristics of included studies

Table 1 shows basic characteristics of the 23 included studies. These studies were published from 2001 to 2024. There were 211 and 214 animals in the intervention and control groups, respectively. In total, 7 studies used BALB/c mice (23–29), 6 studies used C57BL/6 J mice (17, 30–34), 5 studies used nude mice (35–39), 2 studies used laka mice (40, 41), 1 study used severe combined immunodeficient mice (42), 1 study used A/J mice (43), and 1 study used the Rowett nude rat (44). A total of 10 studies (23–25, 28, 30, 31, 35, 37, 42, 43) used female mice, and 7 studies (29, 33–35, 40, 41, 44) used male mice, while the other 7 studies (17, 26, 27, 32, 36, 38, 39) did not report the sex of animals. In addition, 4 studies established mouse models of orthotopic xenograft (40, 41, 43, 44), while the remaining studies used ectopic transplanted tumor mouse models. The dose range of RESV was from 0.23 to 3,000 mg/kg. The duration ranged from 6 to 84 days. The routes of RESV included oral gavage, intratumor injection, intranasal infusion, intravenous injection, and intraperitoneal injection.

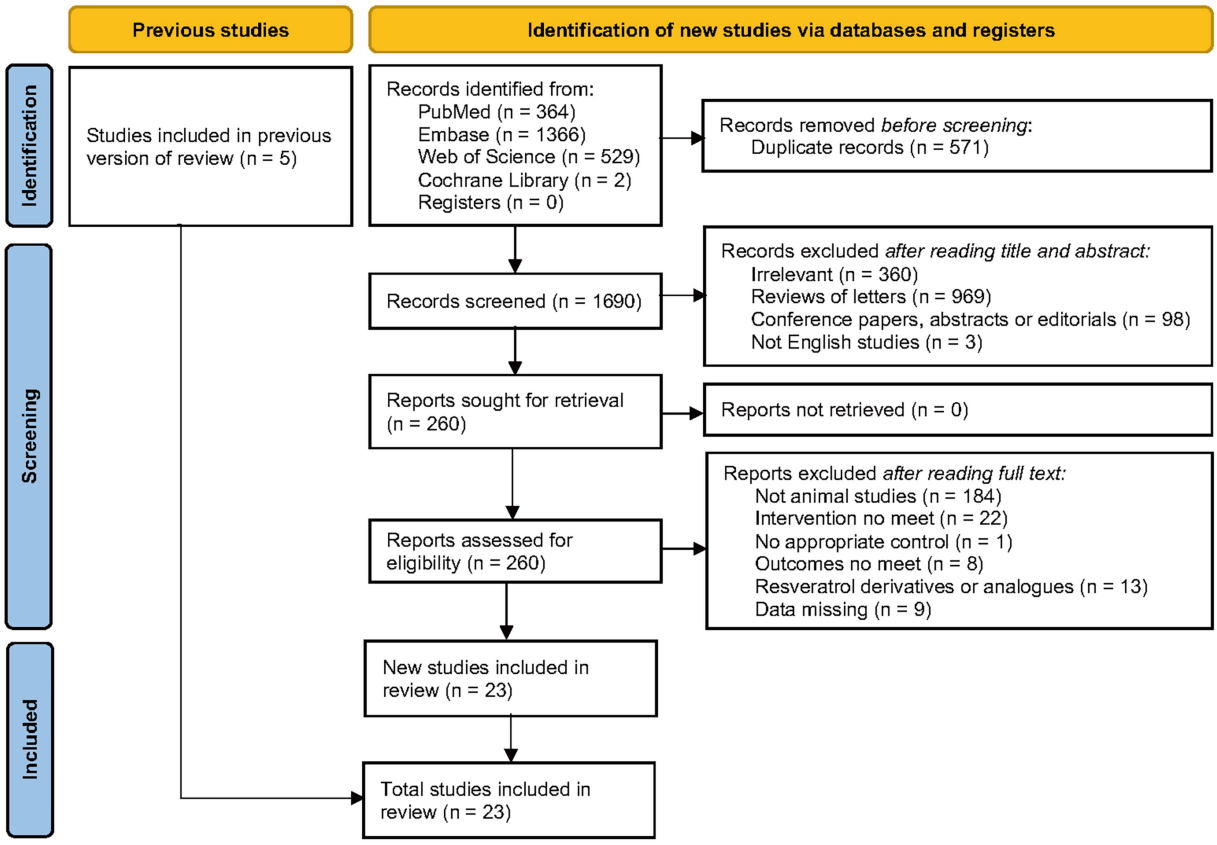

FIGURE 2
Flow chart of the study selection process.

TABLE 1 Basic characteristics of the included studies.

Study	Region	Species (sex, age, *n* = experimental/control group)	Weight (g) (experimental/control group)	Model method (drug/cell, route, dose, duration)	Anesthetic	Intervention (experimental/control group, route)	Dose, duration	Outcomes	*p*-value
Kimura et al. (30)	Japan	C57BL/6 mice (Female, 5, 7/7)	18.8 ± 0.40/18.1 ± 2.51	HTT (LLC, Sc, 5×10^5, once)	NA	RESV+LLC/LLC, Ip	0.6 mg/kg, QD, 21 days	1; 2; 3; 4	1. P > 0.05; 2. $p < 0.05$; 3. $p > 0.05$; 4. $p < 0.05$
Kimura et al. (30)	Japan	C57BL/6 mice (Female, 5, 7/7)	18.5 ± 1.09/18.1 ± 2.51	HTT (LLC, Sc, 5×10^5, once)	NA	RESV+LLC/LLC, Ip	2.5 mg/kg, QD, 21 days	1; 2; 3; 4	1. $p > 0.05$; 2. $p < 0.05$; 3. $p > 0.05$; 4. $p < 0.05$
Kimura et al. (30)	Japan	C57BL/6 mice (Female, 5, 7/7)	18.9 ± 0.74/18.1 ± 2.51	HTT (LLC, Sc, 5×10^5, once)	NA	RESV+LLC/LLC, Ip	10 mg/kg, QD, 21 days	1; 2; 3; 4	1. $p < 0.05$; 2. $p < 0.05$ 3. $p > 0.05$; 4. $p < 0.05$
Lee et al. (31)	Korea	C57BL/6 J mice (Female, 5, 6/6)	NA	HTT (LLC, Sc, 3×10^5/100 μL, once)	NA	RESV+LLC/LLC, Ip	20 mg/kg, QD, 21 days	1; 2; 5	1. $p < 0.001$; 2. $p < 0.01$; 5. $p < 0.05$
Busquets et al. (32)	Spain	C57BL/6 mice (NA, 12, 6/6)	24.7 ± 2.45/25.7 ± 2.69	HTT (LLC, Im, 5×10^5, once)	Ketamine and xylazine	RESV+LLC/LLC, Ip	5 mg/kg, QD, 15 days	1; 2; 3; 4	1. $p > 0.05$; 2. $p > 0.05$ 3. $p > 0.05$; 4. $p < 0.05$
Busquets et al. (32)	Spain	C57BL/6 mice (NA, 12, 6/6)	23.9 ± 1.96/25.7 ± 2.69	HTT (LLC, Im, 5×10^5, once)	Ketamine and xylazine	RESV+LLC/LLC, Ip	25 mg/kg, QD, 15 days	1; 2; 3; 4	1. $p > 0.05$; 2. $p > 0.05$ 3. $p > 0.05$; 4. $p < 0.05$
Malhotra et al. (40)	India	Laka mice (Male, NA, 8/9)	18–20	*In situ* (BaP, Ip, 100 mg/kg, once)	Ether	RESV+BaP/BaP, Ga	5.7 mg/kg, Q2D, 35 days	3	3. $p < 0.05$
Zhao et al. (23)	China	BALB/c mice (Female, NA, 6/6)	18–22	HTT (SPC-A-1-CDDP, Sc, 1×10^8, once)	NA	RESV+SPC-A-1-CDDP/SPC-A-1-CDDP, NA	1,000 mg/kg, QD, 28 days	1; 2	1. $p < 0.05$; 2. $p < 0.05$
Zhao et al. (23)	China	BALB/c mice (Female, NA, 6/6)	18–22	HTT (SPC-A-1-CDDP, Sc, 1×10^8, once)	NA	RESV+SPC-A-1-CDDP/SPC-A-1-CDDP, NA	3,000 mg/kg, QD, 28 days	1; 2	1. $p < 0.05$; 2. $p < 0.05$
Malhotra et al. (41)	India	Laka mice (Male, NA, 8/9)	18–20	In situ (BaP, Ip, 100 mg/kg, once)	Ether	RESV+BaP/BaP, Ga	5.7 mg/kg, TW, 22 days	3	3. $p < 0.001$
Vetvicka et al. (24)	USA	BALB/c mice (Female, 8, 5/5)	NA	HTT (LLC, Im, 5×10^5, once)	CO_2	RESV+LLC/LLC, Ip	5 mg/kg, QD, 15 days	4	4. $p > 0.05$
Yin et al. (35)	China	Nude mice (Male & Female, 6–8, 6/6)	18–22	HTT (A549, Sc, 5×10^6, once)	NA	RESV+A549/A549, Iv	15 mg/kg, QD, 15 days	1; 3	1. $p < 0.05$; 3. $p > 0.05$
Yin et al. (35)	China	Nude mice (Male and Female, 6–8, 6/6)	18–22	HTT (A549, Sc, 5×10^6, once)	NA	RESV+A549/A549, Iv	30 mg/kg, QD, 15 days	1; 3	1. $p < 0.01$; 3. $p > 0.05$
Yin et al. (35)	China	Nude mice (Male and Female, 6–8, 6/6)	18–22	HTT (A549, Sc, 5×10^6, once)	NA	RESV+A549/A549, Iv	60 mg/kg, QD, 15 days	1; 3	1. $p < 0.01$; 3. $p > 0.05$

(Continued)

10.3389/fnut.2025.1644538

TABLE 1 (Continued)

Study	Region	Species (sex, age, *n* = experimental/control group)	Weight (g) (experimental/control group)	Model method (drug/cell, route, dose, duration)	Anesthetic	Intervention (experimental/control group, route)	Dose, duration	Outcomes	*p*-value
Yu et al. (42)	China	SCI mice (Female, 4–6, 10/10)	NA	HTT (A549-FOXC2, Sc, 2×10^6, once)	NA	RESV+A549-FOXC2/A549-FOXC2, Ip	20 mg/kg, QD, 42 days	1	1. $p < 0.05$
Yu et al. (42)	China	SCI mice (Female, 4–6, 10/10)	NA	HTT (A549, Sc, 2×10^6, once)	NA	RESV+A549/A549, Ip	20 mg/kg, QD, 42 days	1	1. $p > 0.05$
Bai et al. (36)	China	Nude mice (NA, 6–8, 15/15)	NA	HTT (H460, Sc, 3×10^7/200 µl, once)	CO_2	RESV+H460/H460, Ii	200 µl, B2D, 15 days	1; 2	1. $p < 0.05$; 2. $p < 0.05$
Vetvicka et al. (25)	USA	BALB/c mice (Female, 8, 5/5)	NA	HTT (LLC, Im, 5×10^6, once)	CO_2	RESV+LLC/LLC, Ga	5 mg/kg, QD, 14 days	4	4. $p < 0.05$
Li et al. (37)	China	Nude mice (Female, 5, 5/5)	NA	HTT (H460, Sc, 1×10^6/100 µl, once)	NA	RESV+H460/H460, Ip	30 mg/kg, Q3D, 8 days	1; 2	1. $p < 0.05$; 2. $p < 0.05$
He et al. (38)	China	Nude mice (NA, NA, 5/5)	NA	HTT (A549, Iv, 1×10^7/200 µl, once)	NA	RESV+A549/A549, Ip	10 mg/kg, QD, 14 days	4	4. $p > 0.05$
Sun et al. (17)	China	C57BL/6 mice (NA, 4–5, 5/5)	NA	HTT (LLC, Sc, 1×10^6, once)	Ketamine and xylazine	RESV+LLC/LLC, Ip	100 mg/kg, QD, 28 days	1; 2	1. $p < 0.01$; 2. $p < 0.01$
Monteillier et al. (43)	Switzerland	A/J mice (Female, 5–6, 14/14)	14–16	In situ (NNK, Ip, 50 mg/kg, QW, 2doses)	NA	RESV+NNK/NNK, Nasal	80 mg/kg, TW, 26 days	1; 3	1. $p < 0.01$; 3. $p < 0.05$
Zhao et al. (33)	China	C57BL/6 mice (Male, 6–8, 6/6)	NA	HTT (LLC, Sc, 1×10^6/200 µl, once)	NA	RESV+LLC/LLC, Ga	50 mg/kg, QD, 21 days	2	2. $p < 0.01$
Song et al. (26)	China	BALB/c mice (NA, 6–8, 8/8)	NA	HTT (HCC827, Sc, 1×10^6/100 µl, once)	NA	RESV+HCC827/HCC827, Iv	50 mg/kg, Q3D, 6 days	1; 2	1. $p < 0.05$; 2. $p < 0.05$
Zheng et al. (27)	China	BALB/c mice (NA, 4–6, 5/5)	NA	HTT (A549, Sc, 2×10^6, once)	NA	RESV+A549/A549, Iv	15 mg/kg, Q3D, 15 days	1; 2	1. $p < 0.001$; 2. $p > 0.05$
Qin et al. (39)	China	Nude mice (NA, NA, 5/5)	NA	HTT (HCC827, Sc, 2×10^6/200 µl, once)	NA	RESV+HCC827/HCC827, Iv	0.23 mg/kg, 5 times/week, 25 days	1; 2	1. $p < 0.01$; 2. $p > 0.05$
Wang et al. (44)	China	Rowett nude rats (Male, 8, 8/8)	240–260	In situ (A549, Nasal, 2×10^7, once)	Sodium pentobarbital and isoflurane	RESV+A549/A549, Ga	250 mg/kg, QD, 84 days	3; 5	3. $p > 0.05$; 5. $p < 0.05$
Antonio et al., 2021	Spain	BALB/c mice (Female, 10, 10/10)	20	HTT (LP07, Sc, 4×10^5/200 µl, once)	Sodium pentobarbital	RESV+LP07/LP07, Ip	20 mg/kg, QD, 15 days	2; 3	2. $p < 0.05$; 3. $p < 0.001$
Savio et al. (34)	Italy	C57BL/6 J mice (Male, 4, 5/6)	NA	HTT (LLC, Sc, 1×10^6/400 µL, once)	NA	RESV+LLC/LLC, Ga	125 mg/kg, QD, 21 days	1; 2; 5	1. $p < 0.05$; 2. $p > 0.05$; 5. $p < 0.001$
Liang et al. (29)	China	BALB/c mice (Male, 8–10, 5/5)	20 ± 1	HTT (A549, Sc, 5×10^6/200 µl, once)	CO_2	RESV+A549/A549, Ip	10 mg/kg, QD, 28 days	1; 2	1. $p < 0.001$; 2. $p < 0.01$

B2D, Twice every 2 days; BaP, benzo[a]pyrene; FOXC2, Forkhead Box C2; Ga, Gavage; HTT, Heterotopic tumor transplantation; Ii, Intratumor injection; Ip, Intraperitoneal; Iv, Intravenous injection; LC, Lung cancer; LLC, Lewis lung cancer; NA, Not available; NNK, 4-(N-methyl-N-nitrosamino)-1-(3-pyridyl)-1-butanone; QD, Quaque die; Q2D, Quaque secunda die; Q3D, Quaque tertia die; RESV, Resveratrol; Sc, Subcutaneous injection; SCI, Severe combined Immunodeficient; TW, Three times a week; 1, Tumor volume; 2. Tumor weight; 3. Body weight; 4. Lung metastases number; 5. Apoptotic cell proportion.

10.3389/fnut.2025.1644538

Quality of included studies

According to the 10-item CAMARADES checklist, the quality scores of included studies ranged from 3 to 7, with an average score of 4.7 (Figure 3). Two studies received (29, 44) 7 points, three studies received 6 points (28, 34, 36), six studies received 5 points (17, 25, 32, 39–41), 10 studies received 4 points (23, 24, 26, 27, 31, 33, 35, 38, 42, 43), and two studies received 3 points (30, 37). All studies reported detailed information on animal models, and 22 studies reported compliance with animal welfare regulations and statements of potential conflicts of interest. However, no studies have reported the application of blindness and sample size calculation.

Intervention effects

Primary outcomes

Tumor volume

Data from 313 mice (156 in the intervention group and 157 in the control group) from 22 experiments showed that RESV significantly reduced tumor volume of LC [SMD = −2.44, 95% CI (−3.16, −1.71), $p < 0.00001$]. High heterogeneity was observed among the experiments ($I^2 = 80\%$, $p < 0.00001$; Figure 4A).

Tumor weight

A total of 18 experiments with 241 mice (120 in the intervention group and 121 in the control group) revealed a significant reduction of tumor weight of LC [SMD = −1.30, 95% CI (−2.07, −0.52), $p = 0.001$]. The heterogeneity analysis showed high heterogeneity among the 18 experiments ($I^2 = 83\%$, $p < 0.00001$; Figure 4B).

Secondary outcomes

Lung metastases number

A total of 8 experiments with 96 mice (48 in the intervention group and 48 in the control group) indicated that RESV significantly decreased the lung metastases number of LC [SMD = −1.15, 95% CI (−1.61, −0.69), $p < 0.00001$]. There was low heterogeneity among the experiments ($I^2 = 0\%$, $p = 0.50$; Figure 5A).

Body weight

A total of 13 experiments with 200 mice (99 in the intervention group and 101 in the control group) indicated that RESV increased the body weight of LC mice, while the difference was not statistically significant [SMD = 0.37, 95% CI (−0.25, 0.99), $p = 0.25$]. There was moderate heterogeneity among the experiments ($I^2 = 75\%$, $p < 0.00001$; Figure 5B).

Apoptotic cell proportion

A total of 3 experiments with 39 mice (19 in the intervention group and 20 in the control group) indicated that RESV significantly increased apoptotic cell proportion of LC cells [SMD = 5.97, 95% CI (0.87, 11.06), $p = 0.02$]. High heterogeneity was observed ($I^2 = 88\%$, $p = 0.0003$; Figure 5C).

Exploration of heterogeneity sources

Due to the observed heterogeneity across studies, we used tumor volume as the standardized measurement indicator. First, to assess the robustness of our findings, we performed a leave-one-out sensitivity analysis by sequentially excluding individual trials. The results indicated that after omitting each experiment one by one, the pooled effect estimate did not change significantly, suggesting that the observed heterogeneity could not be attributed to any specific experiment (Figure 6A). Subsequently, we performed subgroup analysis on 21 experiments [excluding Bai et al. (36), due to unreported RESV dosage] stratified by dose ranges, which reduced the overall heterogeneity from high ($I^2 = 80\%$, $p < 0.00001$) to medium ($I^2 = 71\%$, $p < 0.01$). The results showed that the heterogeneities were moderate in the ≤10 mg/kg ($I^2 = 53\%$, $p = 0.06$), 11–20 mg/kg ($I^2 = 64\%$, $p = 0.02$), and >100 mg/kg groups ($I^2 = 71\%$, $p = 0.04$), and the heterogeneities were high in the 21–30 mg/kg ($I^2 = 81\%$, $p < 0.01$) and the 50–100 mg/kg groups ($I^2 = 82\%$, $p < 0.01$; Figure 6B). We observed that the heterogeneity in the ≤10 mg/kg group was mainly caused by the result of Liang et al. (29) and the heterogeneity decreased after deleting this experiment ($I^2 = 0\%$, $p = 0.77$; Figure 6C). Furthermore, we conducted meta-regression analysis to explore the potential heterogeneity source (Table 2). The results suggested that the eight factors (publication year, dose, duration, administration, modeling method, species, gender, and region) were not a source of heterogeneity ($p > 0.05$). Consequently, the observed heterogeneity across studies may be partially attributable to variations in RESV dosage.

Publication bias

We conducted funnel plots and Egger's test to assess publication bias of three outcomes: (1) tumor volume; (2) tumor weight; and (3) body weight. The results showed significant publication bias in 22 studies focusing on tumor volume ($P_{egger} = 0.028$; Figure 7A), and no significant bias in 18 studies focusing on tumor weight ($P_{egger} = 0.262$; Figure 7B) and 13 studies focusing on body weight ($P_{egger} = 0.066$; Figure 7C).

Dose–duration–effect 3D model

To identify the most effective RESV dose and duration for preclinical LC, we conducted a dose–duration–effect 3D model of primary outcomes. One study (23) with a significantly large RESV dose (1,000 and 3,000 mg/kg), which was quite different from other studies, was excluded. Additionally, one study (44) that used rats and another study (36) that reported unclear RESV dose (200 μL) were also excluded. Hence, the RESV dose used for the 3D model was from 0.23 to 125 mg/kg. The tumor volume was significantly suppressed when the dose of RESV was no less 30 mg/kg, and the treatment lasted for 25–28 days (Figure 8A). Furthermore, in studies where tumor weight was significantly reduced, the duration of RESV treatment was predominantly concentrated within 21–28 days, with doses typically ranging from 30 to 100 mg/kg (Figure 8B). Thus, the optimized dose and duration of RESV for LC were 30–100 mg/kg and 25–28 days.

Toxicology of RESV

RESV demonstrates potential nephrotoxicity (59% probability) and cardiotoxicity (51% probability), with no other organ toxicity and no toxicity endpoint shown (Table 3). Furthermore, the predicted toxicity class was 4, and the predicted LD50 of RESV was 1,560 mg/kg, which was higher than most of the doses in available studies.

Discussion

Primary findings

Previous meta-analysis evaluated the effect of RESV on the incidence of LC tumors (19). However, it failed to comprehensively evaluate the efficacy and safety of RESV on LC. With the publication of a large number of preclinical studies in recent years, we conducted this updated meta-analysis to systematically evaluate the efficacy and safety of RESV for LC in multiple dimensions, including tumor volume, tumor weight, lung metastases number, body weight, and apoptotic cell proportion. Moreover, the toxicological characteristics and optimal dose and duration of RESV were explored. To be specific, 30 experiments from 23 studies were synthesized, and the quality of the included studies was moderate. RESV significantly reduced tumor volume, tumor weight, and lung metastases number, and increased the apoptotic cell proportion, while it could not improve the body weight of mice. High heterogeneities were observed in primary outcomes, and the dose of RESV may be a potential heterogeneity source. The suggested dose and duration of RESV for LC mice were 30–100 mg/kg and 25–28 days, while the LD50 of RESV was 1,560 mg/kg, indicating that RESV was safe for LC mice.

Heterogeneity

The considerable heterogeneity observed in tumor volume may be attributable to multiple confounding variables across the included trials, including variations in experimental methodologies (modeling techniques, administration protocols, and treatment duration), pharmacological parameters (RESV dosage and formulation), and biological factors (animal species and sex), in addition to potential temporal trends reflected by publication year. *A priori*, we anticipated substantial heterogeneity given these methodological variations. Subsequent subgroup stratification by RESV dose partly reduced heterogeneity metrics, suggesting dosage variation as a partial explanatory factor. However, residual heterogeneity persisted despite comprehensive meta-regression analyses, implying the potential influence of unmeasured covariates. These may include inter-laboratory environmental differences, instrumentation variability, and technical artifacts in image-based data extraction processes.

Potential mechanism of RESV for LC

Decrease the viability of the LC cells

Figure 9 shows the mechanism of RESV for LC. RESV decreased the viability of LC cells through regulating cell cycle, aging, and epithelial–mesenchymal transition (EMT). RESV maintained the A549 cell cycle in the G1 phase and altered the expression of cyclin A, Chk1, CDC27, and Eg5 (45). In another study, RESV induced a concentration-dependent stagnation of the A549 cell cycle in the S phase, which was associated with the inhibition of retinoblastoma protein phosphorylation and the upregulation of the cyclin-dependent kinase inhibitor p21WAF1/CIP (46). Furthermore, RESV induced the expression of NADPH oxidase-5 in A549 and H460 cells, which promoted reactive oxygen species (ROS) production and upregulated senescence-associated β-galactosidase (SA-β-gal), p53, and p21, resulting in DNA double-strand breaks of LC cells (47). In addition, RESV increased ROS in LC cells by inducing mitochondrial dysfunction, leading to the upregulation of aging-related molecules, including p38MAPK, p27, p21, and RB (48). Moreover, RESV reduced TGF-β-induced EMT by increasing E-cadherin and decreasing fibronectin, vimentin, SNAIL, and SLUG (49). Meanwhile, RESV

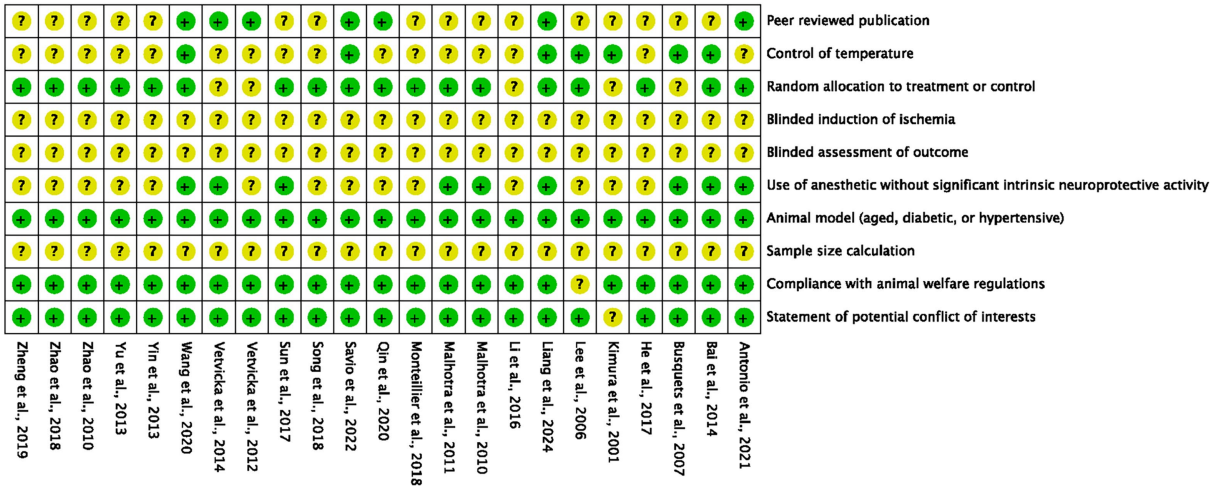

FIGURE 3
Risk of bias assessment of included studies.

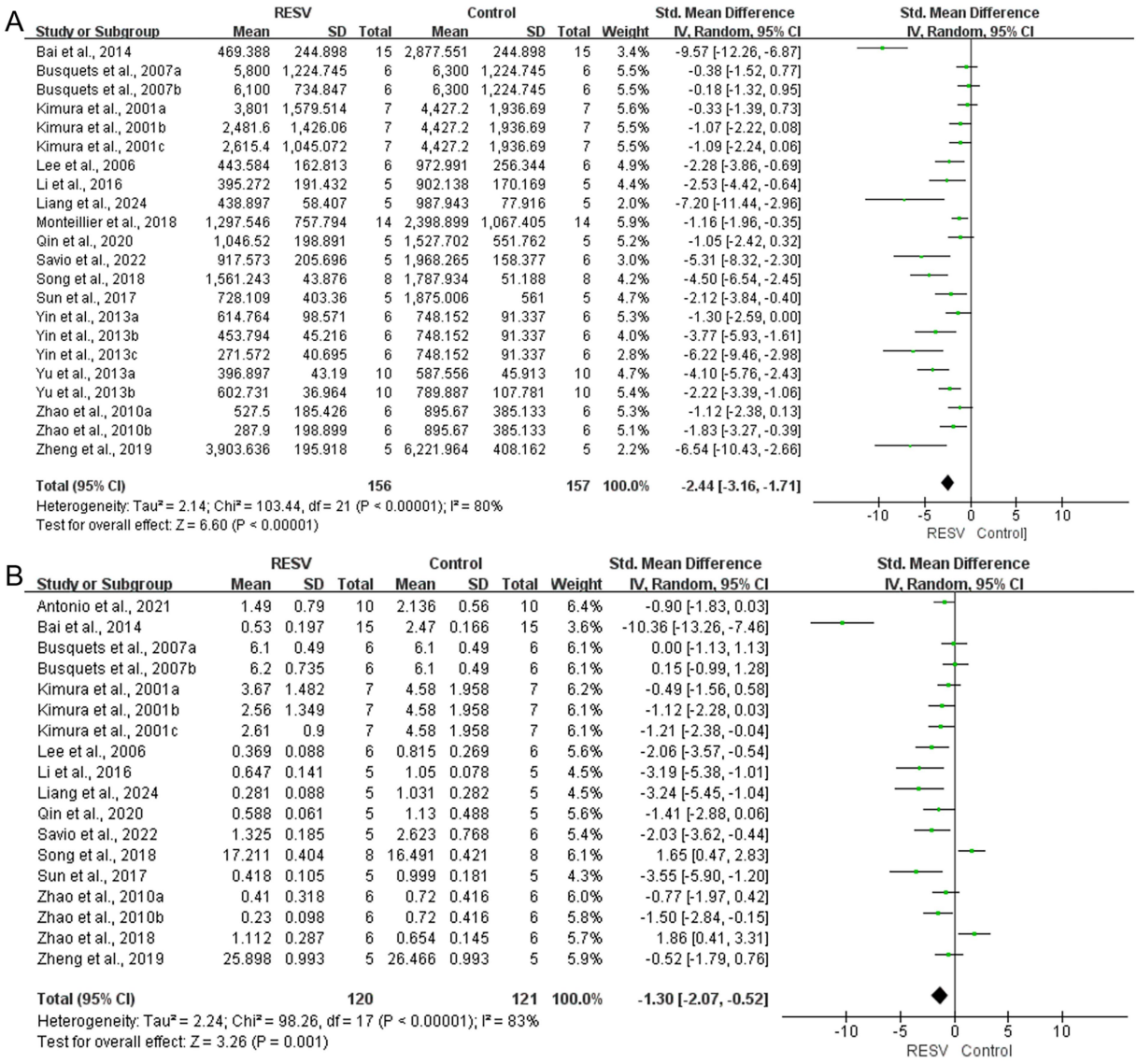

FIGURE 4
The meta-analysis result of the effect of RESV on primary outcomes of LC. **(A)** Tumor volume (mm^3); **(B)** Tumor weight (g).

suppressed FOXC2, a critical regulator of EMT, by influencing miRNA-520 h-mediated signaling pathways (42).

Promote apoptosis and autophagy of LC cell

Apoptosis and autophagy are gene-controlled programmed cell death and degradation pathways that contribute to maintaining cell homeostasis (50). RESV inhibited Nrf2, NQO1, and SOD1 in a dose-and time-dependent way to destroy the antioxidant pool and induce ROS, thereby promoting the apoptosis of LC cells (51). In addition, RESV promoted the transfer of apoptosis-inducing factor from cytoplasm to nucleus by increasing ROS and decreasing mitochondrial membrane potential, thereby promoting the apoptosis of LC cells (52). Meanwhile, RESV induced apoptosis by decreasing protein arginine methyltransferase 5 through inhibiting the Akt/GSK3β pathway (53). Furthermore, RESV activated caspase 8 and decreased c-FLIP, p-EGFR, and p-Akt in H460 cells, thereby promoting apoptosis (54). RESV increased NGFR mRNA expression and prolonged NGFR mRNA and protein survive, then activated AMPK-mTOR pathway to promote autophagy and apoptosis of A549 cells (55). Additionally, RESV inhibited the Akt/mTOR pathway and activated the p38-MAPK pathway by upregulating SIRT1, thereby inducing apoptosis and autophagy of LC cells (56).

Regulate tumor immune microenvironment

The heterogeneity of the immune microenvironment is related to the progression and treatment responsiveness of cancer. RESV significantly increased the expression of programmed cell death ligand 1 in NCI-H358 cells, which plays a vital role in suppressing T-cell-mediated immune responses (57). Triacetylresveratrol, a RESV analog, is a potent SIRT2 agonist and is associated with the infiltration of multiple immune cells in LC, including CD8 + T cells, CD4 + T cells, CD4 + memory resting, regulatory T cells, and natural killer cells (58). Furthermore, RESV enhanced the cytotoxic

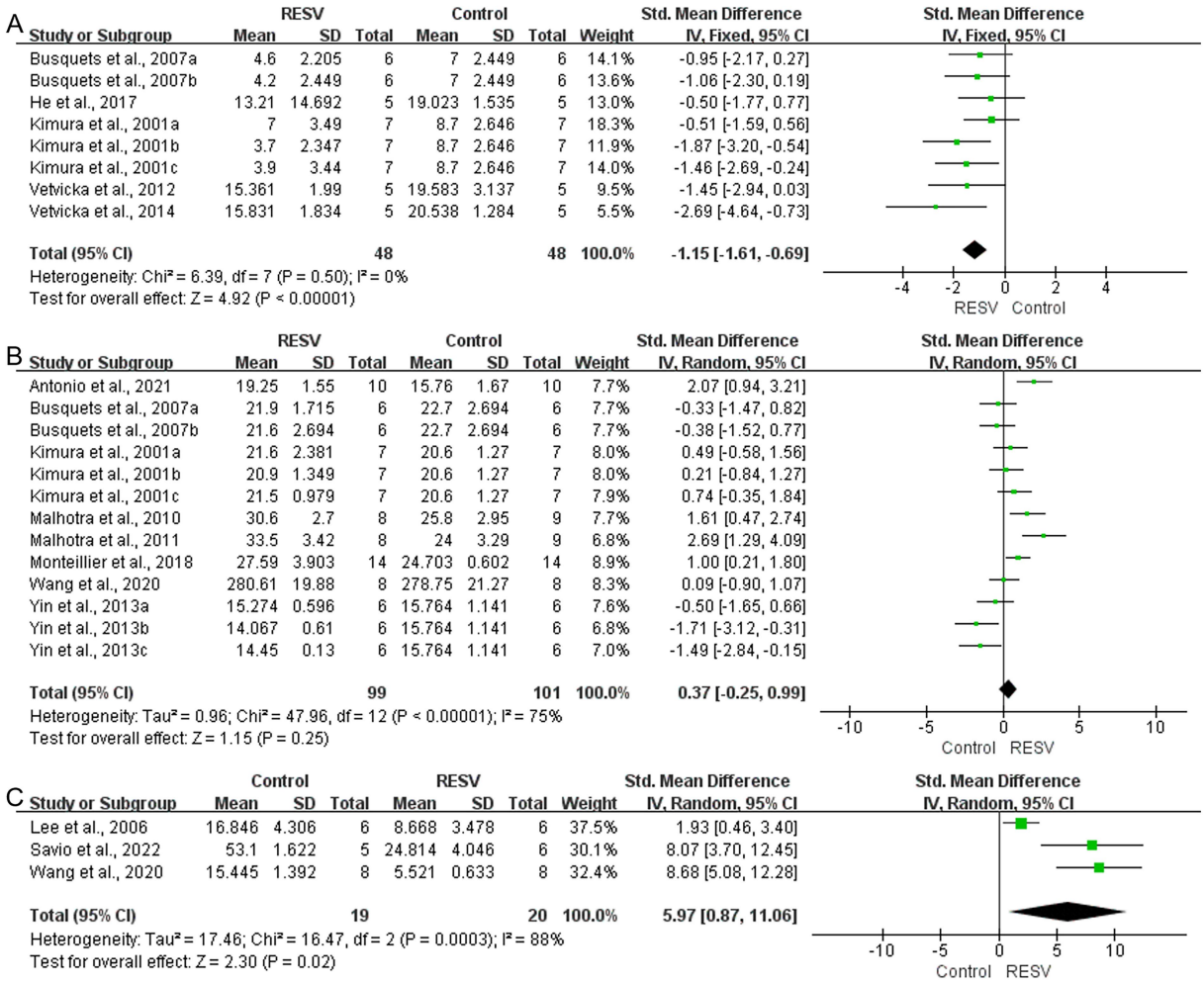

FIGURE 5
The meta-analysis result of the effect of RESV on secondary outcomes of LC. **(A)** Lung metastases number; **(B)** Body weight (g); **(C)** Apoptotic cell proportion (%).

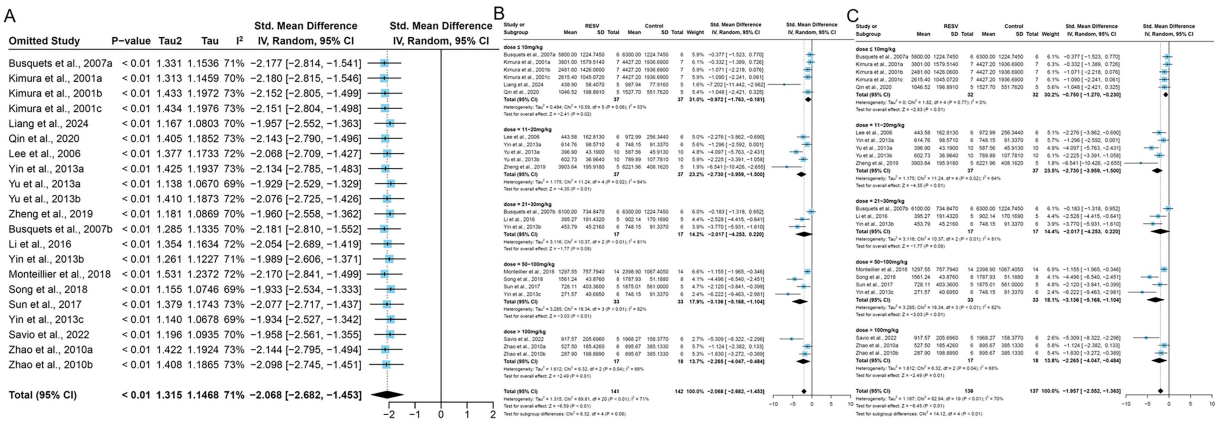

FIGURE 6
The subgroup and sensitivity analysis of RESV on tumor volume (mm^3) of LC. **(A)** Forest plot of leave-one-out sensitivity analysis; **(B)** Forest plot of tumor volume [subgroup analysis by dose of RESV after removing Bai et al. (36)]; **(C)** Forest plot of tumor volume [subgroup analysis by dose of RESV after removing Liang et al. (29)].

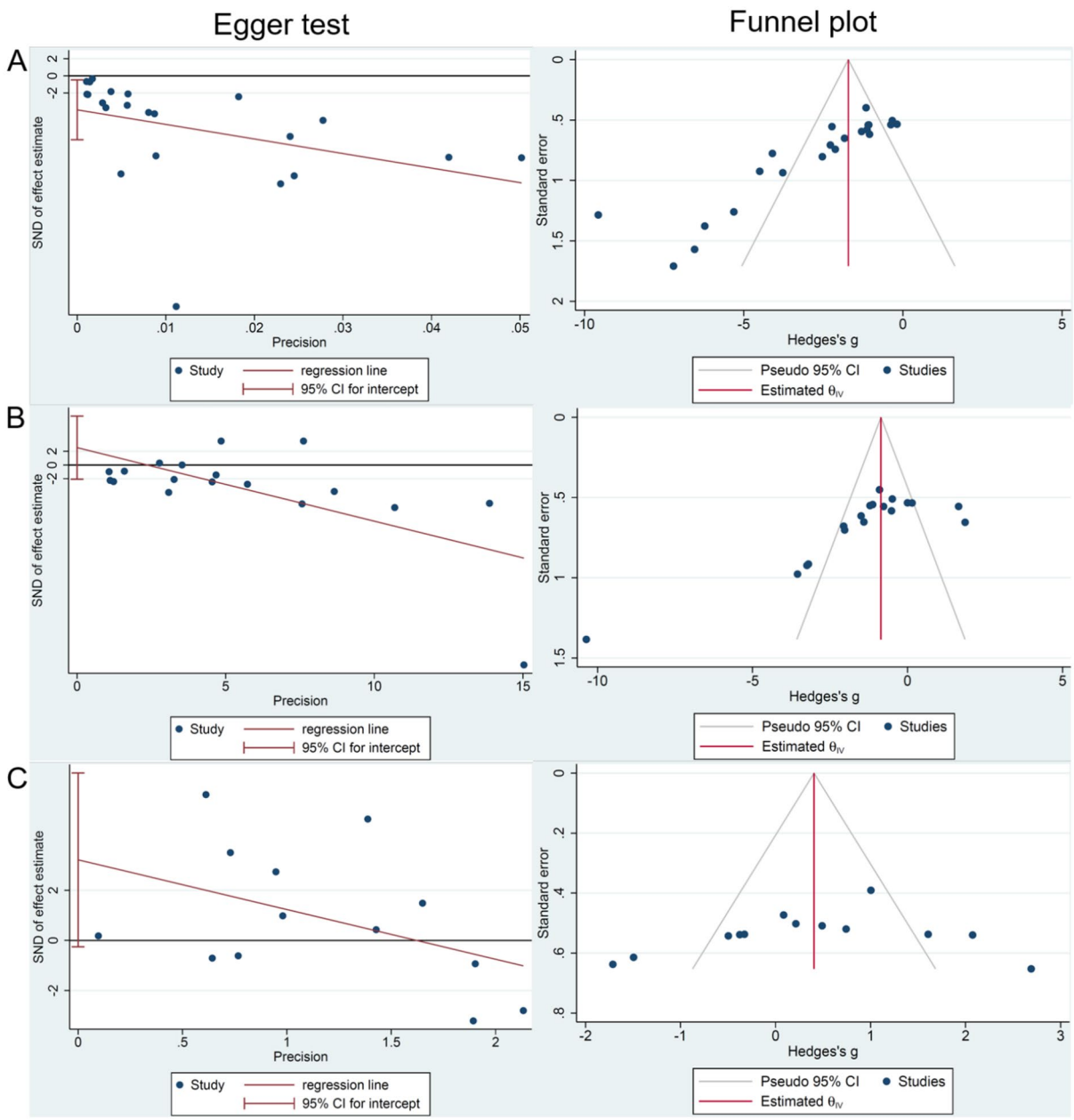

FIGURE 7
The publication bias analysis of RESV on LC. **(A)** Tumor volume (mm^3); **(B)** Tumor weight (g); **(C)** Body weight (g).

TABLE 2 Elucidate the source of the heterogeneity using meta-regression.

Factor	*P* > |t|	95% CIs	
Publication year	1.00	−0.08	0.08
Dose	1.00	−0.22	0.22
Duration	1.00	−0.23	0.23
Administration	1.00	−0.52	0.52
Modeling method	0.39	−1.41	3.41
Species	1.00	−0.33	0.33
Sex	1.00	−0.43	0.43
Region	1.00	−0.28	0.28

of CD8 + T cells, the most important cytotoxic immune cells, by modulating the SLC7A11-HMMR interaction and activating ferroptosis (59). Moreover, RESV downregulated STAT3 *in vitro*, thereby inhibiting M2-like polarization of tumor-associated macrophages (TAMs) and suppressing the proliferation of LC cells (17). In another study, TAM (CD68+) infiltration in LC tumors, including tumor-promoting M2 macrophages (CD163+) and lymphocytes (CD3+), was significantly reduced after RESV treatment (34). In addition, RESV promoted the secretion of IL-18 by regulating TAMs in LC, and IL-18 was a key cytokine that promoted the activation of CD8 + T cells (60). RESV prevented the transformation of normal fibroblasts into cancer-associated fibroblasts (CAFs) through regulating autophagy, thus disrupting the promotion of LC by CAFs (34).

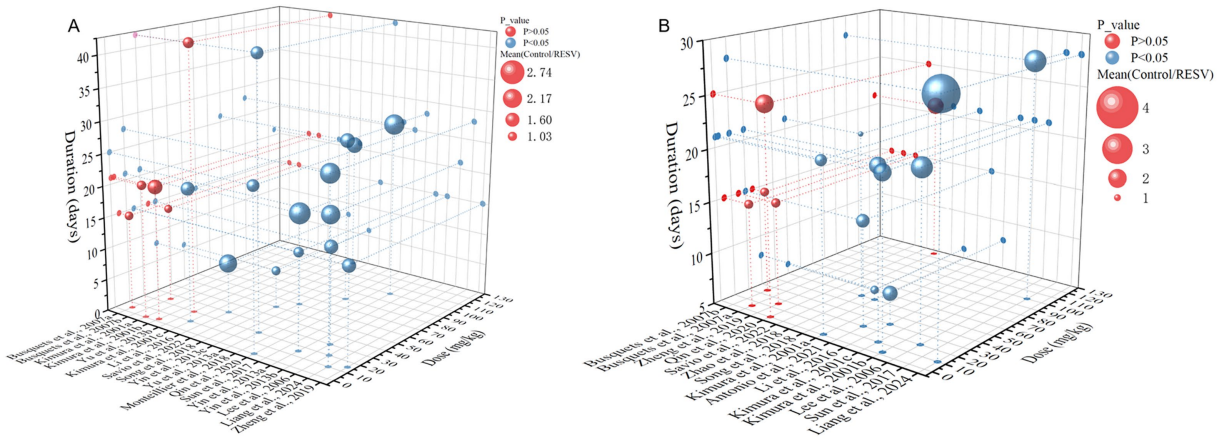

FIGURE 8
The dose–duration–effect 3D model of RESV treating LC. **(A)** Tumor volume (mm^3); **(B)** tumor weight (g).

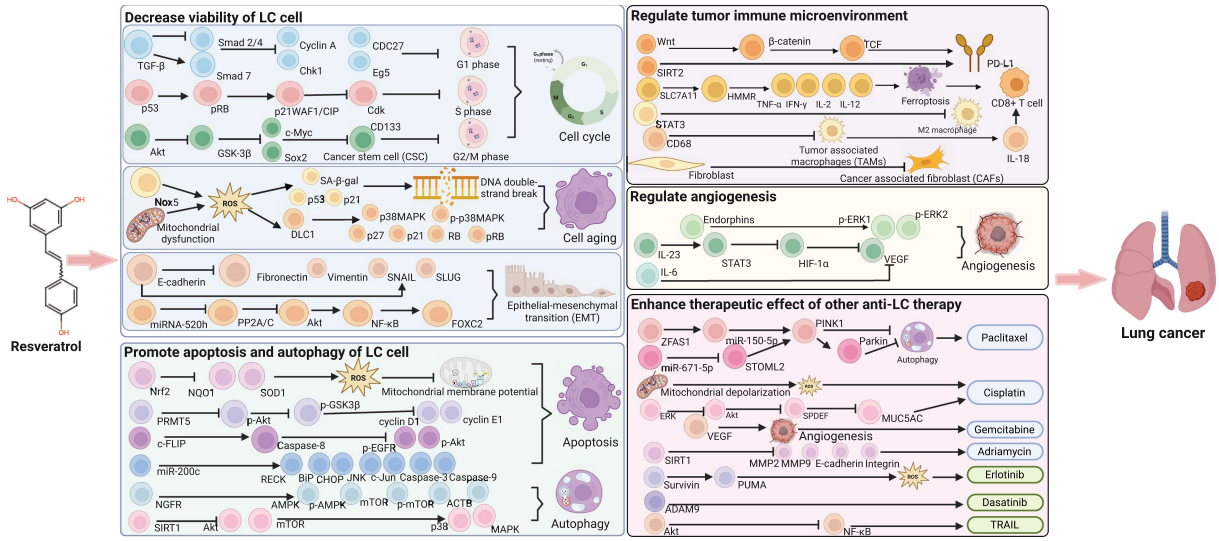

FIGURE 9
Potential mechanism of RESV for LC (created using BioRender.com).

Regulate angiogenesis

Angiogenesis is a crucial mechanism by which tumor cells acquire nutrients and metastasize. However, angiogenesis has been proven to be beneficial for enhancing the efficacy of anti-LC treatment. For instance, RESV reduced endorphins and increased phosphorylated ERK 1/2, thereby promoting microvessel growth and tumor blood perfusion. Under such conditions, the cytotoxic effect of gemcitabine on LC cells was significantly enhanced (39). In H460 cells, RESV downregulates VEGF expression, which is an important regulator of microvascular production (54). In another study, RESV regulated angiogenesis by inhibiting the STAT3/HIF-1α/VEGF pathway (44). In addition, RESV significantly inhibited the secretion of cytokines IL-6 and VEGF in co-cultured A549 cells and mesenchymal stem cells (61). *In vivo* studies showed that RESV reduced the expression of the angiogenic marker CD31 in tumor tissues (34). In small-cell LC, IL-23-induced inflammatory microenvironment activated the STAT3/VEGF pathway, whereas RESV inhibited this activation (62).

Enhance the therapeutic effect of other anti-LC therapies

A large number of studies showed that RESV was a promising anti-LC adjuvant. RESV inhibited autophagy of A549 cells by regulating ZFAS1/miR-150-5p/PINK1 pathway, thereby enhancing the sensitivity of LC to paclitaxel (63). Meanwhile, RESV enhanced the susceptibility of A549 cells to paclitaxel through miR-671-5p-mediated inhibition of STOML2 (64). RESV enhanced the effect of cisplatin on mitochondrial apoptosis of small-cell LC by promoting mitochondrial depolarization and ROS production (65). RESV regulated the SPDEF-MUC5AC axis by inhibiting ERK and Akt

TABLE 3 Evaluation of toxicological parameters of RESV through ProTox-3.0.

Classification	Target	Prediction	Probability
Organ toxicity	Hepatotoxicity	Inactive	0.74
Organ toxicity	Neurotoxicity	Inactive	0.77
Organ toxicity	Nephrotoxicity	Active	0.59
Organ toxicity	Respiratory toxicity	Inactive	0.57
Organ toxicity	Cardiotoxicity	Active	0.51
Toxicity endpoints	Carcinogenicity	Inactive	0.71
Toxicity endpoints	Immunotoxicity	Inactive	0.86
Toxicity endpoints	Mutagenicity	Inactive	0.92
Toxicity endpoints	Cytotoxicity	Inactive	0.98
Toxicity endpoints	BBB	Inactive	0.55
Toxicity endpoints	Ecotoxicity	Inactive	0.55
Toxicity endpoints	Clinical toxicity	Inactive	0.60
Toxicity endpoints	Nutritional toxicity	Inactive	0.89

signaling, thereby increasing the sensitivity of LC to cisplatin (10). Moreover, RESV enhanced the inhibitory effect of gemcitabine on tumor growth by promoting tumor microvascular growth (39). Meanwhile, RESV decreased SIRT1, MMP2, MMP9, E-cadherin, and integrin in A549 cells to enhance the cytotoxic of adriamycin (66). RESV induced ROS production by downregulating survivin and upregulating PUMA, thereby promoting erlotinib-mediated LC cell apoptosis (67). RESV promoted ADAM9 degradation in LC cells through the ubiquitin–proteasome pathway, thereby enhancing the therapeutic effect of dasatinib on LC cells (68). In A549 and HCC-15 cells, RESV reduced LC resistance to tumor necrosis factor-related apoptosis-inducing ligand by inhibiting the Akt/NF-κB pathway (69). Finally, RESV increased the sensitivity of LC to radiotherapy by upregulating ROS and SA-β-gal in A549 and H460 cells and promoting DNA double-strand breaks (70).

Limitations

Several noteworthy limitations should be acknowledged in this study. First, the generalizability of our findings is constrained by substantial heterogeneity and moderate-to-low methodological quality across included studies. While subgroup analyses and meta-regression identified RESV dosage as a potential source of heterogeneity, residual variability may be explained by additional confounding factors such as experimental conditions and measurement instrumentation. Second, the toxicity predictions generated by ProTox-3.0 require empirical validation through experimental approaches, such as histopathological examination and serum biomarker analysis in preclinical models. Third, despite demonstrating promising clinical potential, the therapeutic application of RESV remains limited by its unfavorable pharmacokinetic properties, notably poor oral bioavailability and rapid systemic metabolism, which pose significant challenges for clinical translation.

Mechanistic investigation and clinical translation challenges of RESV in LC treatment

The mechanistic underpinnings of RESV in LC treatment necessitate further preclinical investigation. Notably, the therapeutic efficacy of RESV against LC is modulated by multiple variables, including dosage, duration, and administration route. Herein, we systematically evaluated the interrelationships among quantifiable parameters (dose, duration, and therapeutic effect) to establish the potentially optimal dosage and duration of RESV in LC-bearing mouse models. The administration route was excluded due to its inherent non-quantifiable nature and inability to account for heterogeneity sources. However, subsequent researches are encouraged to comprehensively apply our findings to explore more appropriate administration routes, which would significantly contribute to systematically optimizing preclinical protocols for RESV-based LC therapy. More importantly, there are other crucial issues that must be addressed prior to clinical translation. RESV exhibits rapid metabolic clearance in humans, undergoing extensive first-pass metabolism in the liver and intestine, where it is converted to inactive sulfate conjugates, resulting in notably low systemic bioavailability (16). To optimize RESV's anti-LC efficacy in human applications, key pharmacological parameters, including formulation, dosage regimen, and administration route, require systematic optimization. While our study identified 30–100 mg/kg as the optimal dose range in animal models, subsequent studies must establish the human equivalent dose through appropriate scaling methods. Furthermore, since mouse models are unable to fully replicate the human tumor microenvironment or pharmacokinetics, it must be recognized that the optimal dose and duration proposed in this study cannot simply be applied to human research through equivalent dose conversion. Previous clinical investigations have demonstrated that micronized formulations can enhance RESV bioavailability by approximately threefold compared to conventional preparations, achieved through increased surface area and improved suspension properties (71). Current preclinical research has focused extensively on RESV nanoparticle development for LC therapy. These engineered formulations improve bioavailability through multiple mechanisms, such as enhancing aqueous solubility, improving chemical stability, controlling release kinetics, and targeted delivery (16). Although still in preclinical development, RESV nanoparticles demonstrate promising translational potential. While clinical evaluation of RESV for LC treatment represents a crucial next step, rigorous resolution of these pharmacological challenges is imperative to ensure patient safety and therapeutic efficacy. The transition to human trials must be predicated on comprehensive preclinical data addressing these fundamental issues.

Conclusion

As a safe food-derived compound, RESV can effectively inhibit LC tumor growth *in vivo*, especially to control tumor volume, tumor weight, lung metastasis number, and tumor cell apoptosis rate. Its action mechanism is complex and may be related to regulating cell cycle, cell senescence, EMT, apoptosis, autophagy, angiogenesis, and immune microenvironment. However, the clinical research on RESV treatment of LC is limited, which is the key research field to promote the clinical application of RESV.

Data availability statement

The original contributions presented in the study are included in the article/Supplementary material, further inquiries can be directed to the corresponding authors.

Author contributions

XX: Formal analysis, Conceptualization, Validation, Writing – original draft, Data curation, Investigation, Writing – review & editing. XW: Methodology, Data curation, Investigation, Conceptualization, Writing – review & editing, Writing – original draft, Formal analysis. WL: Investigation, Writing – review & editing, Writing – original draft, Methodology, Data curation. FY: Writing – original draft, Writing – review & editing, Supervision. JG: Investigation, Funding acquisition, Validation, Project administration, Writing – review & editing, Supervision, Writing – original draft, Methodology.

Funding

The author(s) declare that financial support was received for the research and/or publication of this article. This study was supported by the National Natural Science Foundation of China (No. 82305188); the China Postdoctoral Science Foundation (No. 2022MD723715); and the Natural Science Foundation of Sichuan Science and Technology Department (No. 23NSFSC6246).

Acknowledgments

The authors thank BioRender for their outstanding contributions to biological picture rendering.

Conflict of interest

The authors declare that the research was conducted in the absence of any commercial or financial relationships that could be construed as a potential conflict of interest.

Generative AI statement

The authors declare that no Gen AI was used in the creation of this manuscript.

Any alternative text (alt text) provided alongside figures in this article has been generated by Frontiers with the support of artificial intelligence and reasonable efforts have been made to ensure accuracy, including review by the authors wherever possible. If you identify any issues, please contact us.

Publisher's note

Supplementary material

The Supplementary material for this article can be found online at: https://www.frontiersin.org/articles/10.3389/fnut.2025.1644538/full#supplementary-material

References

1. Bray F, Laversanne M, Sung H, Ferlay J, Siegel RL, Soerjomataram I, et al. Global cancer statistics 2022: GLOBOCAN estimates of incidence and mortality worldwide for 36 cancers in 185 countries. *CA Cancer J Clin*. (2024) 74:229–63. doi: 10.3322/caac.21834

2. Bai X, Liu Y, Cao Y, Ma Z, Chen Y, Guo S. Exploring the potential of cryptochlorogenic acid as a dietary adjuvant for multi-target combined lung cancer treatment. *Phytomedicine*. (2024) 132:155907. doi: 10.1016/j.phymed.2024.155907

3. Liu K, Li Q, Lu X, Fan X, Yang Y, Xie W, et al. Seven oral traditional Chinese medicine combined with chemotherapy for the treatment of non-small cell lung cancer: a network meta-analysis. *Pharm Biol*. (2024) 62:404–22. doi: 10.1080/13880209.2024.2351940

4. Ganti AK, Klein AB, Cotarla I, Seal B, Chou E. Update of incidence, prevalence, survival, and initial treatment in patients with non-small cell lung Cancer in the US. *JAMA Oncol*. (2021) 7:1824–32. doi: 10.1001/jamaoncol.2021.4932

5. Suzuki-Chiba H, Konishi T, Aso S, Makito K, Matsui H, Jo T, et al. Comparison of olanzapine 2.5 mg and 5 mg in the prevention of chemotherapy-induced nausea and vomiting: a Japanese nationwide database study. *Int J Clin Oncol*. (2024) 29:1762–73. doi: 10.1007/s10147-024-02603-2

6. Ohmori T, Yamaoka T, Ando K, Kusumoto S, Kishino Y, Manabe R, et al. Molecular and clinical features of EGFR-TKI-associated lung injury. *Int J Mol Sci*. (2021) 22:792. doi: 10.3390/ijms22020792

7. Lahiri A, Maji A, Potdar PD, Singh N, Parikh P, Bisht B, et al. Lung cancer immunotherapy: progress, pitfalls, and promises. *Mol Cancer*. (2023) 22:40. doi: 10.1186/s12943-023-01740-y

8. Tian B, Liu J. Resveratrol: a review of plant sources, synthesis, stability, modification and food application. *J Sci Food Agric*. (2020) 100:1392–404. doi: 10.1002/jsfa.10152

9. Singh N, Nagar E, Gautam A, Kapoor H, Arora N. Resveratrol mitigates mi R-212-3p mediated progression of diesel exhaust-induced pulmonary fibrosis by regulating SIRT1/fox O3. *Sci Total Environ*. (2023) 902:166063. doi: 10.1016/j.scitotenv.2023.166063

10. Lin YH, Zhu LY, Yang YQ, Zhang ZH, Chen QG, Sun YP, et al. Resveratrol inhibits MUC5AC expression by regulating SPDEF in lung cancer cells. *Phytomedicine*. (2021) 89:153601. doi: 10.1016/j.phymed.2021.153601

11. Behroozaghdam M, Dehghani M, Zabolian A, Kamali D, Javanshir S, Hasani Sadi F, et al. Resveratrol in breast cancer treatment: from cellular effects to molecular mechanisms of action. *Cell Mol Life Sci*. (2022) 79:539. doi: 10.1007/s00018-022-04551-4

12. Zhang Z, Ji Y, Hu N, Yu Q, Zhang X, Li J, et al. Ferroptosis-induced anticancer effect of resveratrol with a biomimetic nano-delivery system in colorectal cancer treatment. *Asian J Pharm Sci*. (2022) 17:751–66. doi: 10.1016/j.ajps.2022.07.006

13. Wang L, Wang Y, Xie Q, Xu S, Yang C, Liu F, et al. Resveratrol liposomes reverse sorafenib resistance in renal cell carcinoma models by modulating PI3K-AKT-mTOR and VHL-HIF signaling pathways. *Int J Pharm X*. (2024) 8:100280. doi: 10.1016/j.ijpx.2024.100280

14. Wang Y, Su L, Hu Z, Peng S, Li N, Fu H, et al. Resveratrol suppresses liver cancer progression by downregulating AKR1C3: targeting HCC with HSA nanomaterial as a carrier to enhance therapeutic efficacy. *Apoptosis*. (2024) 29:1429–53. doi: 10.1007/s10495-024-01995-w

15. Khan K, Quispe C, Javed Z, Iqbal MJ, Sadia H, Raza S, et al. Resveratrol, curcumin, paclitaxel and mi RNAs mediated regulation of PI3K/Akt/mTOR pathway: go four better to treat bladder cancer. *Cancer Cell Int*. (2020) 20:560. doi: 10.1186/s12935-020-01660-7

16. Najafiyan B, Bokaii Hosseini Z, Esmaelian S, Firuzpour F, Rahimipour Anaraki S, Kalantari L, et al. Unveiling the potential effects of resveratrol in lung cancer treatment: mechanisms and nanoparticle-based drug delivery strategies. *Biomed Pharmacother*. (2024) 172:116207. doi: 10.1016/j.biopha.2024.116207

17. Sun L, Chen B, Jiang R, Li J, Wang B. Resveratrol inhibits lung cancer growth by suppressing M2-like polarization of tumor associated macrophages. *Cell Immunol*. (2017) 311:86–93. doi: 10.1016/j.cellimm.2016.11.002

18. Geng Q, Yan L, Shi C, Zhang L, Li L, Lu P, et al. Therapeutic effects of flavonoids on pulmonary fibrosis: a preclinical meta-analysis. *Phytomedicine*. (2024) 132:155807. doi: 10.1016/j.phymed.2024.155807

19. Feng Y, Zhou J, Jiang Y. Resveratrol in lung cancer-a systematic review. *J BUON*. (2016) 21:950–3.

20. Page MJ, McKenzie JE, Bossuyt PM, Boutron I, Hoffmann TC, Mulrow CD, et al. The PRISMA 2020 statement: an updated guideline for reporting systematic reviews. *BMJ*. (2021) 372:n71. doi: 10.1136/bmj.n71

21. Macleod MR, O'Collins T, Howells DW, Donnan GA. Pooling of animal experimental data reveals influence of study design and publication bias. *Stroke*. (2004) 35:1203–8. doi: 10.1161/01.STR.0000125719.25853.20

22. Wu X, Xiao X, Chen X, Yang M, Hu Z, Shuai S, et al. Effectiveness and mechanism of metformin in animal models of pulmonary fibrosis: a preclinical systematic review and meta-analysis. *Front Pharmacol*. (2022) 13:13. doi: 10.3389/fphar.2022.948101

23. Zhao W, Bao P, Qi H, You H. Resveratrol down-regulates survivin and induces apoptosis in human multidrug-resistant SPC-A-1/CDDP cells. *Oncol Rep*. (2010) 23:279–86.

24. Vetvicka V, Vetvickova J. Combination of glucan, resveratrol and vitamin C demonstrates strong anti-tumor potential. *Anticancer Res*. (2012) 32:81–7.

25. Vetvicka V, Vetvickova J. Natural immunomodulators and their stimulation of immune reaction: true or false? *Anticancer Res*. (2014) 34:2275–82.

26. Song Z, Shi Y, Han Q, Dai G. Endothelial growth factor receptor-targeted and reactive oxygen species-responsive lung cancer therapy by docetaxel and resveratrol encapsulated lipid-polymer hybrid nanoparticles. *Biomed Pharmacother*. (2018) 105:18–26. doi: 10.1016/j.biopha.2018.05.095

27. Zheng Q, Cheng W, Zhang X, Shao R, Li Z. A pH-induced reversible assembly system with resveratrol-controllable loading and release for enhanced tumor-targeting chemotherapy. *Nanoscale Res Lett*. (2019) 14:305. doi: 10.1186/s11671-019-3139-z

28. Penedo-Vázquez A, Duran X, Mateu J, López-Postigo A, Barreiro E. Curcumin and resveratrol improve muscle function and structure through attenuation of proteolytic markers in experimental Cancer-induced Cachexia. *Molecules*. (2021) 26:4904. doi: 10.3390/molecules26164904

29. Liang G, Peng H, Lu S, Li Y, Yang N. Resveratrol exerts inhibitory effects on the growth and metastasis of lung Cancer and modulates the polarization of tumor-associated neutrophils. *J Biol Regul Homeost Agents*. (2024) 38:4185–96. doi: 10.23812/j.biol.regul.homeost.agents.20243805.332

30. Kimura Y, Okuda H. Resveratrol isolated from *Polygonum cuspidatum* root prevents tumor growth and metastasis to lung and tumor-induced neovascularization in Lewis lung carcinoma-bearing mice. *J Nutr*. (2001) 131:1844–9. doi: 10.1093/jn/131.6.1844

31. Lee EO, Lee HJ, Hwang HS, Ahn KS, Chae C, Kang KS, et al. Potent inhibition of Lewis lung cancer growth by heyneanol a from the roots of *Vitis amurensis* through apoptotic and anti-angiogenic activities. *Carcinogenesis*. (2006) 27:2059–69. doi: 10.1093/carcin/bgl055

32. Busquets S, Ametller E, Fuster G, Olivan M, Raab V, Argilés JM, et al. Resveratrol, a natural diphenol, reduces metastatic growth in an experimental cancer model. *Cancer Lett*. (2007) 245:144–8. doi: 10.1016/j.canlet.2005.12.035

33. Zhao Y, Shao Q, Zhu H, Xu H, Long W, Yu B, et al. Resveratrol ameliorates Lewis lung carcinoma-bearing mice development, decreases granulocytic myeloid-derived suppressor cell accumulation, and impairs its suppressive ability. *Cancer Sci*. (2018) 109:2677–86. doi: 10.1111/cas.13720

34. Savio M, Ferraresi A, Corpina C, Vandenberghe S, Scarlata C, Sottile V, et al. Resveratrol and its analogue 4, 4'-Dihydroxy-trans-stilbene inhibit Lewis lung carcinoma growth in vivo through apoptosis, autophagy and modulation of the tumour microenvironment in a murine model. *Biomedicine*. (2022) 10:1784. doi: 10.3390/biomedicines10081784

35. Yin HT, Tian QZ, Guan L, Zhou Y, Huang XE, Zhang H. *In vitro* and *in vivo* evaluation of the antitumor efficiency of resveratrol against lung cancer. *Asian Pac J Cancer Prev*. (2013) 14:1703–6. doi: 10.7314/apjcp.2013.14.3.1703

36. Bai T, Dong DS, Pei L. Synergistic antitumor activity of resveratrol and mi R-200c in human lung cancer. *Oncol Rep*. (2014) 31:2293–7. doi: 10.3892/or.2014.3090

37. Li W, Ma X, Li N, Liu H, Dong Q, Zhang J, et al. Resveratrol inhibits hexokinases II mediated glycolysis in non-small cell lung cancer via targeting Akt signaling pathway. *Exp Cell Res*. (2016) 349:320–7. doi: 10.1016/j.yexcr.2016.11.002

38. He L, Fan F, Hou X, Gao C, Meng L, Meng S, et al. Resveratrol suppresses pulmonary tumor metastasis by inhibiting platelet-mediated angiogenic responses. *J Surg Res*. (2017) 217:113–22. doi: 10.1016/j.jss.2017.05.009

39. Qin SH, Lau ATY, Liang ZL, Tan HW, Ji YC, Zhong QH, et al. Resveratrol promotes tumor microvessel growth via Endoglin and extracellular signal-regulated kinase signaling pathway and enhances the anticancer efficacy of gemcitabine against lung Cancer. *Cancer*. (2020) 12:974. doi: 10.3390/cancers12040974

40. Malhotra A, Nair P, Dhawan DK. Modulatory effects of curcumin and resveratrol on lung carcinogenesis in mice. *Phytother Res*. (2010) 24:1271–7. doi: 10.1002/ptr.3087

41. Malhotra A, Nair P, Dhawan DK. Curcumin and resveratrol synergistically stimulate p 21 and regulate cox-2 by maintaining adequate zinc levels during lung carcinogenesis. *Eur J Cancer Prev*. (2011) 20:411–6. doi: 10.1097/CEJ.0b013e3283481d71

42. Yu YH, Chen HA, Chen PS, Cheng YJ, Hsu WH, Chang YW, et al. MiR-520h-mediated FOXC2 regulation is critical for inhibition of lung cancer progression by resveratrol. *Oncogene*. (2013) 32:431–43. doi: 10.1038/onc.2012.74

43. Monteillier A, Voisin A, Furrer P, Allémann E, Cuendet M. Intranasal administration of resveratrol successfully prevents lung cancer in a/J mice. *Sci Rep*. (2018) 8:14257. doi: 10.1038/s41598-018-32423-0

44. Wang H, Jia R, Lv T, Wang M, He S, Zhang X. Resveratrol suppresses tumor progression via inhibiting STAT3/HIF-1α/VEGF pathway in an Orthotopic rat model of non-small-cell lung Cancer (NSCLC). *Onco Targets Ther*. (2020) 13:7057–63. doi: 10.2147/OTT.S259016

45. Whyte L, Huang YY, Torres K, Mehta RG. Molecular mechanisms of resveratrol action in lung cancer cells using dual protein and microarray analyses. *Cancer Res*. (2007) 67:12007–17. doi: 10.1158/0008-5472.CAN-07-2464

46. Kim YA, Lee WH, Choi TH, Rhee SH, Park KY, Choi YH. Involvement of p21WAF1/CIP1, pRB, Bax and NF-kappa B in induction of growth arrest and apoptosis by resveratrol in human lung carcinoma A549 cells. *Int J Oncol*. (2003) 23:1143–9.

47. Luo H, Yang A, Schulte BA, Wargovich MJ, Wang GY. Resveratrol induces premature senescence in lung cancer cells via ROS-mediated DNA damage. *PLoS One*. (2013) 8:e60065. doi: 10.1371/journal.pone.0060065

48. Bian Y, Wang X, Zheng Z, Ren G, Zhu H, Qiao M, et al. Resveratrol drives cancer cell senescence via enhancing p38MAPK and DLC1 expressions. *Food Funct*. (2022) 13:3283–93. doi: 10.1039/d1fo02365a

49. Wang H, Zhang H, Tang L, Chen H, Wu C, Zhao M, et al. Resveratrol inhibits TGF-β1-induced epithelial-to-mesenchymal transition and suppresses lung cancer invasion and metastasis. *Toxicology*. (2013) 303:139–46. doi: 10.1016/j.tox.2012.09.017

50. Russell RC, Guan KL. The multifaceted role of autophagy in cancer. *EMBO J*. (2022) 41:e110031. doi: 10.15252/embj.2021110031

51. Liang C, Yi K, Zhou X, Li X, Zhong C, Cao H, et al. Destruction of the cellular antioxidant pool contributes to resveratrol-induced senescence and apoptosis in lung cancer. *Phytother Res*. (2023) 37:2995–3008. doi: 10.1002/ptr.7795

52. Li W, Li C, Ma L, Jin F. Resveratrol inhibits viability and induces apoptosis in the small-cell lung cancer H446 cell line via the PI3K/Akt/c-Myc pathway. *Oncol Rep*. (2020) 44:1821–30. doi: 10.3892/or.2020.7747

53. Li Y, Yang Y, Liu X, Long Y, Zheng Y. PRMT5 promotes human lung Cancer cell apoptosis via Akt/Gsk 3β signaling induced by resveratrol. *Cell Transplant*. (2019) 28:1664–73. doi: 10.1177/0963689719885083

54. Wright C, Iyer AKV, Yakisich JS, Azad N. Anti-tumorigenic effects of resveratrol in lung Cancer cells through modulation of c-FLIP. *Curr Cancer Drug Targets*. (2017) 17:669–80. doi: 10.2174/1568009617666170315162932

55. Li J, Fan Y, Zhang Y, Liu Y, Yu Y, Ma M. Resveratrol induces autophagy and apoptosis in non-small-cell lung Cancer cells by activating the NGFR-AMPK-mTOR pathway. *Nutrients*. (2022) 14:2413. doi: 10.3390/nu14122413

56. Wang J, Li J, Cao N, Li Z, Han J, Li L. Resveratrol, an activator of SIRT1, induces protective autophagy in non-small-cell lung cancer via inhibiting Akt/mTOR and activating p38-MAPK. *Onco Targets Ther*. (2018) 11:7777–86. doi: 10.2147/OTT.S159095

57. Maj E, Maj B, Bobak K, Gos M, Chodyński M, Kutner A, et al. Differential response of lung Cancer cells, with various driver mutations, to plant polyphenol resveratrol and vitamin D active metabolite PRI-2191. *Int J Mol Sci*. (2021) 22:2354. doi: 10.3390/ijms22052354

58. He J, Qiu N, Zhou X, Meng M, Liu Z, Li J, et al. Resveratrol analog, triacetylresveratrol, a potential immunomodulator of lung adenocarcinoma immunotherapy combination therapies. *Front Oncol*. (2022) 12:1007653. doi: 10.3389/fonc.2022.1007653

59. Shan G, Minchao K, Jizhao W, Rui Z, Guangjian Z, Jin Z, et al. Resveratrol improves the cytotoxic effect of CD8 +T cells in the tumor microenvironment by regulating HMMR/Ferroptosis in lung squamous cell carcinoma. *J Pharm Biomed Anal*. (2023) 229:115346. doi: 10.1016/j.jpba.2023.115346

60. Zhang W, Zhang R, Chang Z, Wang X. Resveratrol activates CD8+ T cells through IL-18 bystander activation in lung adenocarcinoma. *Front Pharmacol*. (2022) 13:1031438. doi: 10.3389/fphar.2022.1031438

61. Sahin E, Baycu C, Koparal AT, Burukoglu Donmez D, Bektur E. Resveratrol reduces IL-6 and VEGF secretion from co-cultured A549 lung cancer cells and adipose-derived mesenchymal stem cells. *Tumour Biol*. (2016) 37:7573–82. doi: 10.1007/s13277-015-4643-0

62. Hou C, Lu L, Liu Z, Lian Y, Xiao J. Resveratrol reduces drug resistance of SCLC cells by suppressing the inflammatory microenvironment and the STAT3/VEGF pathway. *FEBS Open Bio*. (2021) 11:2256–65. doi: 10.1002/2211-5463.13230

63. Kong F, Xie C, Zhao X, Zong X, Bu L, Zhang B, et al. Resveratrol regulates PINK1/Parkin-mediated mitophagy via the lnc RNA ZFAS1-mi R-150-5p-PINK1 axis, and enhances the antitumor activity of paclitaxel against non-small cell lung cancer. *Toxicol Res*. (2022) 11:962–74. doi: 10.1093/toxres/tfac072

64. Kong F, Zhang L, Zhao X, Zhao L, Wang P, Zhang R, et al. Resveratrol augments paclitaxel sensitivity by modulating mi R-671-5p/STOML2/PINK1/Parkin-mediated autophagy signaling in A549 cell. *J Biochem Mol Toxicol*. (2024) 38:e23557. doi: 10.1002/jbt.23557

65. Li W, Shi Y, Wang R, Pan L, Ma L, Jin F. Resveratrol promotes the sensitivity of small-cell lung cancer H446 cells to cisplatin by regulating intrinsic apoptosis. *Int J Oncol*. (2018) 53:2123–30. doi: 10.3892/ijo.2018.4533

66. Yahayo W, Pongkittiphan V, Supabphol R, Saiyudthong S. Comparative studies of resveratrol, Oxyresveratrol and Dihydrooxyresveratrol on doxorubicin-treated lung Cancer cells. *Asian Pac J Cancer Prev*. (2024) 25:939–49. doi: 10.31557/APJCP.2024.25.3.939

67. Nie P, Hu W, Zhang T, Yang Y, Hou B, Zou Z. Synergistic induction of Erlotinib-mediated apoptosis by resveratrol in human non-small-cell lung Cancer cells by Down-regulating Survivin and up-regulating PUMA. *Cell Physiol Biochem*. (2015) 35:2255–71. doi: 10.1159/000374030

68. Lin YS, Hsieh CY, Kuo TT, Lin CC, Lin CY, Sher YP. Resveratrol-mediated ADAM9 degradation decreases cancer progression and provides synergistic effects in combination with chemotherapy. *Am J Cancer Res*. (2020) 10:3828–37.

69. Rasheduzzaman M, Jeong JK, Park SY. Resveratrol sensitizes lung cancer cell to TRAIL by p 53 independent and suppression of Akt/NF-κB signaling. *Life Sci*. (2018) 208:208–20. doi: 10.1016/j.lfs.2018.07.035

70. Luo H, Wang L, Schulte BA, Yang A, Tang S, Wang GY. Resveratrol enhances ionizing radiation-induced premature senescence in lung cancer cells. *Int J Oncol*. (2013) 43:1999–2006. doi: 10.3892/ijo.2013.2141

71. Ren B, Kwah MXY, Liu C, Ma Z, Shanmugam MK, Ding L, et al. Resveratrol for cancer therapy: challenges and future perspectives. *Cancer Lett*. (2021) 515:63–72. doi: 10.1016/j.canlet.2021.05.001

Glossary

B2D - twice every 2 days

BaP - benzo[a]pyrene

BBB - blood–brain barrier

CAFs - cancer-associated fibroblasts

CI - confidence interval

EMT - epithelial–mesenchymal transition

FOXC2 - forkhead box c2

Ga - gavage

HTT - heterotopic tumor transplantation

Ii - intratumor injection

Ip - intraperitoneal

Iv - intravenous injection

LC - lung cancer

LD50 - median lethal dose

LLC - lewis lung cancer

NA - not available

NNK - 4-(N-methyl-N-nitrosamino)-1-(3-pyridyl)-1-butanone

Q2D - quaque secunda die

Q3D - quaque tertia die

QD - quaque die

RESV - resveratrol

ROS - reactive oxygen species

SA-β-gal - senescence-associated β-galactosidase

Sc - subcutaneous injection

SCI - severe combined Immunodeficient

SMD - standardized mean difference

TAMs - tumor-associated macrophages

TW - three times a week

WMD - weighted mean difference